

# STRUCTURES AND ORIENTATIONAL TRANSITIONS IN THIN SMECTIC FILMS OF TILTED HEXATIC

*P. V. Dolganov, K. I. Belov, V. K. Dolganov, E. I. Demikhov*

*Institute of Solid State Physics, RAS  
142432, Chernogolovka, Moscow Region, Russia*

*B. M. Bolotin*

*Institute of Chemical Reactants and Especially Pure Substances IREA  
107076, Moscow, Russia*

*E. I. Kats\**

*Laue-Langevin Institute  
F-38042, Grenoble, France*

*Landau Institute for Theoretical Physics, RAS  
117940 GSP-1, Moscow, Russia*

Received September 20, 2005

We present detailed systematic studies of structural transformations in thin liquid-crystal films with the transition from the smectic-*C* (Sm*C*) to hexatic (HSm*B*) phase. For the first time, all possible structures reported in the literature are observed for one material (5O.6) at the variation of temperature and thickness. In unusual modulated structures, the equilibrium period of stripes is twice the domain size. We interpret these patterns in the framework of a phenomenological Landau-type theory, as equilibrium phenomena produced by a natural geometric frustration in a system having spontaneous splay distortion.

PACS: 61.30.Eb, 64.70.Md, 68.15.+e

## 1. INTRODUCTION

Spontaneous formations of spatial patterns arise in a wide variety of dynamical processes. Even more spectacularly they are observed in equilibrium situations involving fluids, solids, and liquid crystals. Especially remarkable are free standing smectic films, in which the influence of underlying substrates (often dominating in other systems) can be avoided. These systems provide a realization of many models describing diverse apparently disparate physical phenomena (phase transitions, frustrations, ferro-electricity, and magnetism), and an opportunity to study the crossover from two-dimensional to bulk behavior by drawing films of increasing thickness.

For liquid crystal materials with phase sequences in bulk samples HSm*B* (or crystalline Cr*B*)–Sm*A* the

phase transformations in thin free-standing films are well studied presently [1, 2]. At a temperature  $T_{S1}$  that is about 10 °C above the bulk transition point  $T_C$ , the phase transition occurs only in surface smectic layers. The interior layers remain in the Sm*A* phase. Below  $T_{S1}$ , there are no phase transitions up to the temperature slightly above  $T_C$ . The next transition in the nearest-to-surface layer occurs at the temperature  $T_{S2}$  about 1 °C above  $T_C$ . A sequence of discrete layer-by-layer transitions on cooling may constitute from 2 to 5 transitions. In thick films, the transition of the whole film into the low-temperature phase occurs at  $T \sim T_C$ .

A few words on the nomenclature of tilted hexatic smectics (usually labeled as Sm*F*, Sm*I*) may be helpful here. The tilt direction is along the local bonds in the Sm*I* phase, halfway between two local bonds in the Sm*F* phase, and lies at an intermediate angle in Sm*L* phases. Transitions in the films of tilted smectics in which the high-temperature bulk phase is Sm*C* and

---

\*E-mail: kats@ill.fr

the low-temperature phase is tilted hexatic occur in an essentially different way [3–6]. In this case, no sequence of discrete layer-by-layer transitions is observed. After the surface transition into the hexatic structure, the transformation of the film structure on cooling continues in a broad temperature range. Several characteristic temperatures  $T_i$  may be identified at which qualitative changes of the film texture occur. Similar structure and texture transformations were observed in several smectic materials [3–6]. Therefore, one may expect that these transformations have common physical nature and occur through a universal mechanism. But until now the mechanisms of these structural transformations and the physics behind them remain unclear.

Our motivations in this paper are twofold. First, in Sec. 2, we present detailed systematic studies of structural transformations in thin liquid crystal films with the  $SmC$ -to-hexatic phase transition. We go one step further with respect to the results already known (see, e.g., [3–6]) in our investigation of all possible structures in one material (5O.6) at the variation of temperature and thickness. In addition, in Sec. 3, we rationalize and interpret our observations in the framework of a simple phenomenological model that includes the minimal number of ingredients, i.e., it is just at the border between under-fitting models (those that do not explain the data well) and over-fitting models (those that fit the data too well by using too many parameters). Although our model is a toy model in the sense of caricaturizing some physical features, when properly interpreted, it can yield quite reasonable values for a variety of measured quantities. A more realistic model would not affect our conclusions much, and transparency of treatment is worth a simplification. The concluding section is used to briefly summarize our results and to augment their discussion.

## 2. OBSERVATIONS

The measurements were made on the Schiff's-base compound 4-n-hexyl-N-[4-n-pentyloxy-benzilidene]-aniline (5O.6). The sequence of phase transitions in the bulk sample is  $SmA$ –(50.5 °C)– $SmC$ –(49.5 °C)– $HSmB$ . Below the  $HSmB$  phase, the transition to a tilted hexatic structure ( $SmF$ ) occurs in the bulk sample. Free-standing films were prepared by drawing the liquid crystal in a smectic phase across a circular 4 mm hole in a thin glass plate. The experimental set-up enabled simultaneous optical observations and reflectivity measurements. The thickness of the film was determined by the reflected inten-

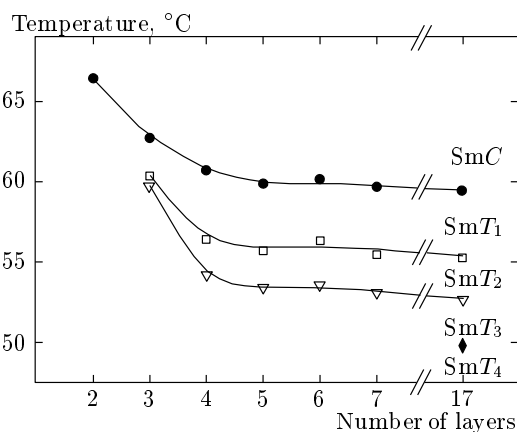


**Fig. 1.** Temperatures of transitions observed in 5O.6 films of different thickness. The high-temperature state corresponds to the  $SmC$  phase. Filled symbols denote structural transitions and open symbols denote transitions associated with change of the director orientation in the film. In thick films ( $N = 17$ ), an additional transition to the  $SmT_4$  state takes place (filled diamond) with a texture typical for the  $SmF$  phase

sity from the film in the «backward» geometry [7]. Observations of the film structure and phase transitions were made using polarized-light reflected microscopy (PRLM) and depolarized-light reflected microscopy (DRLM) [8]. The images were recorded by a CCD camera. The orientational order parameter  $P_2 = (3 \langle \cos^2 \alpha \rangle - 1) / 2$  [9] was determined by optical absorption measurements. At cooling,  $P_2$  changes from 0.75 to 0.8 in the  $SmA$  phase, is about 0.82 in  $SmC$ , and increases up to 0.92 in the hexatic phase.

We performed investigations of thin smectic films starting from the thickness of 2 molecular layers. Figure 1 shows the temperatures of the transitions in the films. Similar symbols denote the temperatures of the transitions between similar structures in the films of different thickness. The high-temperature part of the phase diagram corresponds to the  $SmC$  structure. As was established previously [10], the  $SmC$ – $SmA$  phase transition in free-standing films is essentially shifted to higher temperatures with respect to the bulk samples. The texture of the film is characterized by a smooth spatial variation of the  $c$ -director (Fig. 2a). The picture was taken in the part of the film with a point topological defect, which is typical just for the  $SmC$  phase.

Upon cooling of the  $SmC$  film, the first phase transition (filled circles, the transition into the  $SmT_1$  state, Fig. 1) leads to an abrupt change in the film texture (Fig. 2b). In liquid crystalline materials with the bulk

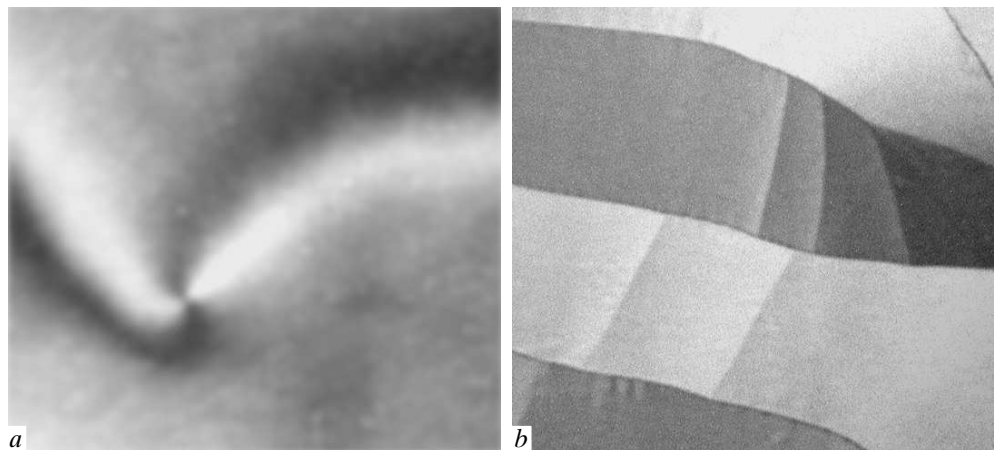


**Fig. 2.** High-temperature textures in a 7-layer film:  $\text{SmC}$ ,  $T = 60.1^\circ\text{C}$  (a),  $\text{SmT}_1$ ,  $T = 59.2^\circ\text{C}$  (b). In frame (a), a point topological defect with characteristic brushes is observed. DRLM. The horizontal size of the frames is about  $420\ \mu\text{m}$

hexatic phases, the higher-temperature transition is associated with the phase transition of the surface layers into the hexatic structure [1, 2]. In thick films, the high-temperature shift of the transition with respect to the phase transition temperature into the  $\text{HSmB}$  structure in the bulk sample is about  $9^\circ\text{C}$ . This value is approximately the same as for the  $\text{HSmB}$ – $\text{SmA}$  transition [1, 2]. A different situation is observed for thin films. For the  $\text{SmA}$  phase, the shift of the transition in the 2-layer film with respect to thick films does not exceed  $2^\circ\text{C}$ , but in our case, this shift is essentially larger (more than  $6^\circ\text{C}$ ). Below the transition, the film consists of domains with different  $\mathbf{c}$ -director orientations and sharp boundaries between them (Fig. 2b). Such a texture may be expected for a tilted hexatic phase in which the  $\mathbf{c}$ -director has a discrete set of orientations and correspondingly sharp boundaries between domains. However, it is not typical for the  $\text{SmC}$  structure, which exists in the interior of the film. For the films with  $N > 5$ , the view of the films is mainly determined by the  $\text{SmC}$  structure of the film interior. Thus, we conclude that the  $\text{SmC}$  structure inside the film differs sufficiently from the conventional  $\text{SmC}$  structure. Sharp boundaries between the domains suggest that the break of the  $\mathbf{c}$ -director orientation occurs not only in the surface layers (i.e., in the hexatic state) but also inside the film (i.e., in the  $\text{SmC}$  state) at the domain boundary. The question arises about the nature of the boundary between the domains inside the film. These peculiarities of the  $\text{SmC}$  structure inside the film become extremely essential after the next transition (open squares in Fig. 1).

At the next transition (into the  $\text{SmT}_2$  state, Figs. 1

and 3), the domains break up into narrow parallel stripes with alternating brightness and sharp boundaries. According to Refs. [3, 4], the surface layers transform under this transition into a so-called  $\text{SmL}$  phase, in which the tilt plane is oriented in the hexatic structure at the angle  $15^\circ$  to the direction of the hexatic bond orientational order. In this structure, 12 equivalent (i.e., having the same energy) orientations of the tilt plane are possible. Our optical measurements confirm that the difference in the  $\mathbf{c}$ -director orientation in the neighboring stripes is about  $30^\circ$  ( $\pm 5^\circ$ ) with two symmetric orientations of the  $\mathbf{c}$ -director relative to the stripe boundary  $\varphi = \pm 15^\circ$  (Fig. 4a–c). The direction of the hexatic bond orientational order does not change across the stripes (along the  $x$  axis), while the direction of the tilt plane changes at the stripe boundary. Inside the film, in the  $\text{SmC}$  structure, there is also a break in the  $\mathbf{c}$ -director orientation. In contrast to this, a smooth change in the stripe orientation along domains is connected with a change in the direction of the bond orientational order, while the orientation of the  $\mathbf{c}$ -director relative to the bond orientational order is preserved. The inset in Fig. 3a clarifies the periodic stripe structure, in particular, in the region of the contact between two stripe domains. The stripe period increases with decreasing the temperature (Fig. 5). When the stripe period achieves the value about  $13$ – $15\ \mu\text{m}$  upon cooling, the stripe width increases sharply and the structure becomes aperiodic. Open triangles in Fig. 1 show the temperatures of this transition.

In the  $\text{SmT}_3$  region (Fig. 1), the film texture may be different (Fig. 3b,c and Fig. 6a) and is similar in many aspects to the material with hexatic phases ob-

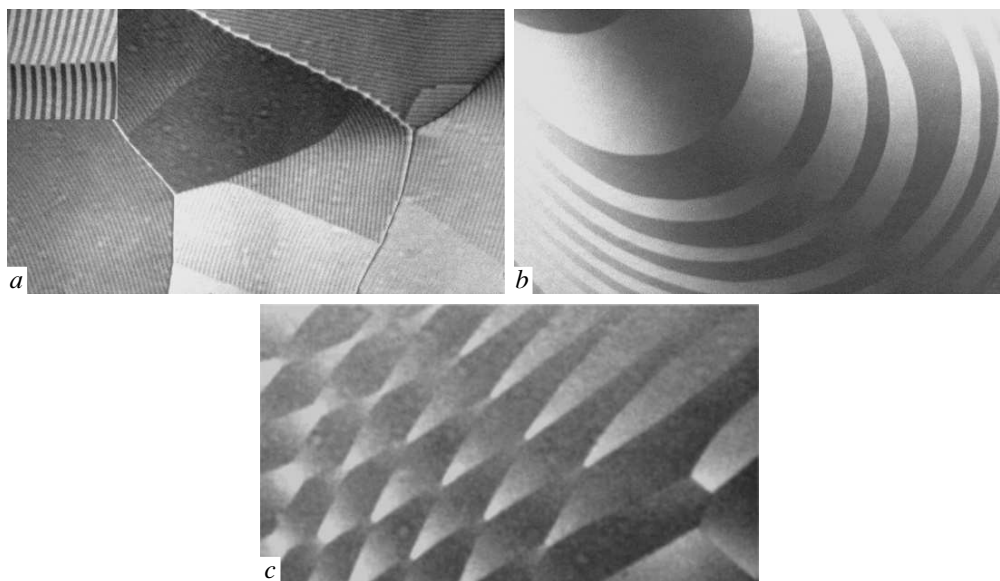


**Fig. 3.** A state with narrow periodic stripes,  $T = 55^\circ\text{C}$ ,  $N = 7$  (a). Inset: stripes in the same film after cooling to  $T = 52.3^\circ\text{C}$ . A structure with linear aperiodic domains,  $T = 51.3^\circ\text{C}$ ,  $N = 17$  (b). A honeycomb texture may form on cooling in a narrow temperature range (c),  $T = 50.8^\circ\text{C}$ ,  $N = 7$ . The horizontal size of frames (a) and (b) is about  $720\ \mu\text{m}$ , frame (c) —  $480\ \mu\text{m}$ , and inset  $160\ \mu\text{m}$ , — DRLM

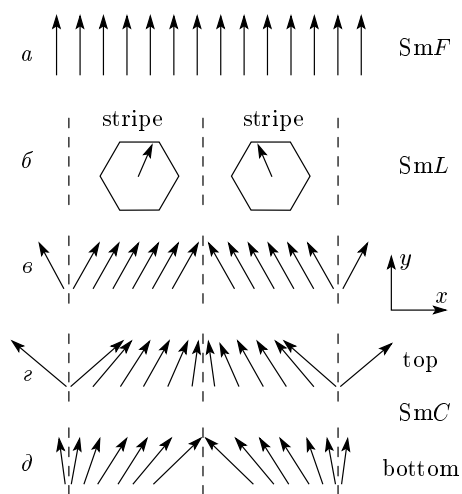


**Fig. 4.** Schematic representation of the stripe structure. Stripes are oriented along the  $y$  axis. (a) Monodomain state ( $\text{Sm}F$ ). (b) In the  $\text{Sm}L$  phase, the  $c$ -director may have two orientations with respect to the bond orientational order ( $\varphi = \pm 15^\circ$ ). (c) Net orientation of the  $c$ -director in the stripes with a jump in the director orientation at the stripe boundary ( $\text{Sm}T_2$  state, Fig. 3a). The structure of the  $\text{Sm}C$  top (d) and bottom (e) layers of the film in the stripe state

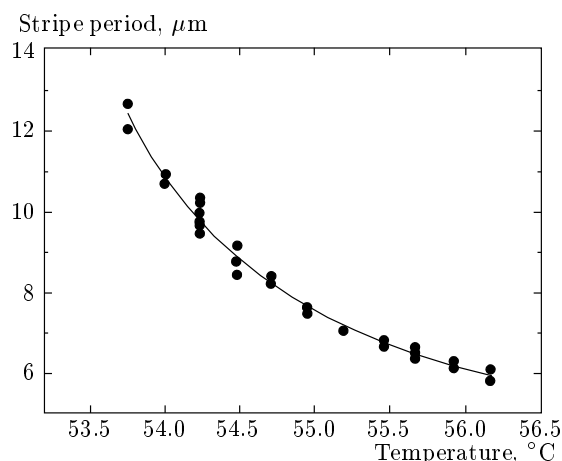


**Fig. 5.** Temperature dependence of the stripe period in a four-layer film. The period monotonically increases with decreasing temperature. The solid line is a fit of the experimental data using Eqs. (3)–(6) with the parameters  $\xi_0/d = 0.5$ ,  $\lambda_0/K = 0.95\ (\mu\text{m})^{-1}$ , and  $\varepsilon/K = 0.61\ (\mu\text{m})^{-1}$

served earlier in  $\text{Sm}C$  films [3–6]. However, the transition temperatures between different textures are hardly reproducible. Moreover, as a rule, the low-temperature texture (Fig. 6a) transforms at heating directly into the state with periodic stripes (Fig. 3a). Therefore, in

the phase diagram (Fig. 1), we indicate only the transition temperature between periodic stripe and aperiodic structures (open triangles in Fig. 1). The domain structure shown in Fig. 3*b* is formed on cooling from the narrow periodic stripes through their broadening. This picture (Fig. 3*b*) was obtained by means of depolarized-light reflection microscopy. The domain boundaries with the same brightness are oriented at about  $45^\circ$  with respect to the polarizers. This manifests the fact that orientations of the  $\mathbf{c}$ -director in the neighboring domains are symmetric with respect to the domain boundary. Measurements with crossed polarizers prove that the  $\mathbf{c}$ -director in the domains is oriented at the angles  $\pm 15^\circ$  with respect to the domain boundary. Therefore, the structure of wide domains (Fig. 3*b*) is similar to the narrow periodic stripes (Fig. 3*a*). The honeycomb texture (Fig. 3*c*) forms from the line domains (Fig. 3*a*) and exists only in a small temperature range (less than  $0.5^\circ\text{C}$ ). More typical textures in the  $\text{SmT}_3$  state are domains with a continuous change in the  $\mathbf{c}$ -director orientation across the domains (the upper part of Fig. 6*a*) or large domains (the lower part of Fig. 6*a*), also with a continuous variation in the  $\mathbf{c}$ -director orientation. In thin films, this structure can be cooled to low temperatures (less than  $40^\circ\text{C}$ ). In thick films ( $N > 10$ ), a reversible phase transition is observed with formation of the texture shown in Fig. 6*c*. This texture is typical for the tilted  $\text{SmF}$  phase. In the limit of very thick films ( $N > 100$ ), crossed domains may be formed (Fig. 6*b*) below the surface phase transition temperature. Two independent sets of domains are formed at both film surfaces. Formation of these independent structures in thick films may indicate that the surface correlation length  $\xi_S$  is less than about 50 smectic interlayer periods.

### 3. THEORETICAL INTERPRETATION

To provide a more complete account of the phenomena described in the previous section, it seems appropriate to discuss how the observed results can be consistently modeled theoretically. Without prior knowledge of the actual structure, we assume the simplest model to answer the natural questions of why the phase transitions in materials with  $\text{SmA}$  and  $\text{SmC}$  phases are so different and what kind of mechanisms are responsible for the formation of the periodic stripe structure and its temperature dependence. From our experimental observations, a few conclusions about the qualitative features of the film structures and their transformations seem inescapable.

First, formation of the periodic stripes (Fig. 3*a*) is related to the structure of the surface layers. In the

higher-temperature  $\text{SmT}_1$  state, the  $\mathbf{c}$ -director is oriented along one direction (Fig. 4*a*) in the middle between apexes of the  $\text{SmF}$  phase hexagon. In the  $\text{SmL}$  phase, the energy minimum splits and the  $\mathbf{c}$ -director may orient in two directions [3, 4] corresponding to two equivalent energy minima ( $\pm 15^\circ$  with respect to the initial orientation, Fig. 4*a,b*). As is known, competing attractive and repulsive interactions generate domain patterns in a wide variety of systems [11]. Formation of a periodic structure is a signature of instability that arises from a competition between two antagonistic fields, and also indicates that above some threshold, a modulated state has a lower energy than the uniform one. In liquid crystals, this scenario is often related to the existence of electric polarization and a certain competition between the long-range forces (the electric and elastic ones). In the thin film under consideration, the electric polarization may appear due to a nonuniform profile of the order parameter induced by the film surface and also because the surface layers are in the hexatic phase. This polarization  $P_l$  is longitudinal (i.e., parallel to the tilt plane) and points in the opposite directions in the upper and lower parts of the film [12–14]. These interactions (electrostatic and elastic) contribute differently to the energy of alternative configurations associated with the existence of domain walls, and may lead to stabilization of the equilibrium stripe period (as in solid-crystal ferroelectric domains).

In liquid crystal films with the broken polar symmetry, there is also another cause of the stripe formation [15–21]. Indeed, the broken polar symmetry allows the terms that are linear in the spatial gradients to occur in the Landau-type free energy expansion. These terms affect the elastic constants, which may even tend to zero. In this situation, the free energy of the defect structure may become more favorable than the uniform structure. Thus, the uniformly ordered state becomes unstable with respect to the striped phase with periodic domain walls. The equilibrium modulated structure arises to optimize the gain in the elastic energy of the orientational deformation inside the stripes and the energy cost to have the defect.

In the literature devoted to theoretical descriptions of the modulated phases in smectic films, models for polar smectic liquid-crystal films with transverse polarization are mostly discussed [16–20]. Apparently, this is not the case for our system. There are several distinctions between the stripes shown in Fig. 3*a* (also see their schematic representation in Fig. 4*b,c*) and the periodic stripes discussed in [16–21]. First, in our case, the structure of the surface layers is hexatic and it dictates the value of director jump at the do-

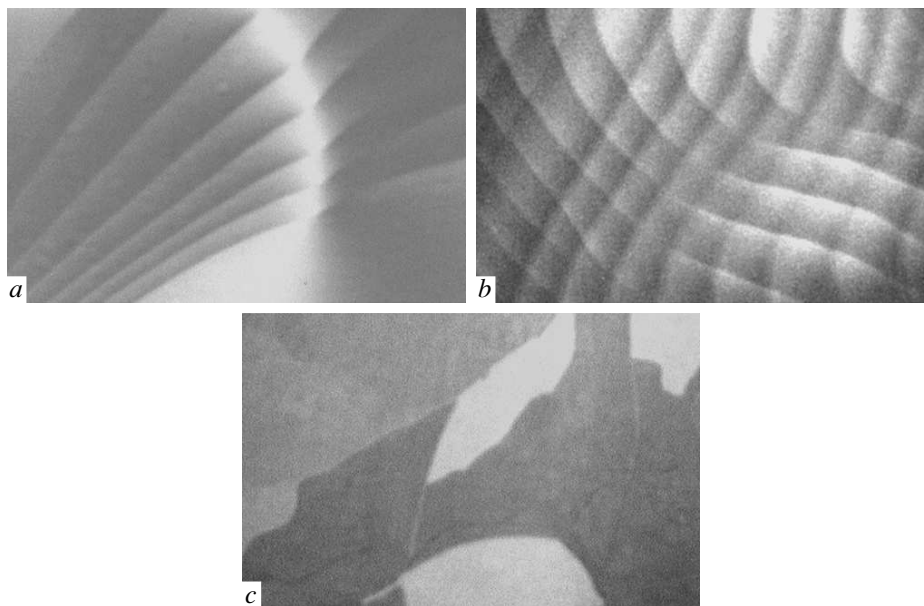


**Fig. 6.** Structures formed in films at low temperatures. Aperiodic domains,  $N = 7$ ,  $T = 50.8^\circ\text{C}$  (*a*). Two sets of crossing domains in a thick film,  $N = 200$ ,  $T = 49.1^\circ\text{C}$  (*b*). On further cooling, a transition to the SmF structure occurs (*c*)  $N = 17$ ,  $T = 48.1^\circ\text{C}$ , DRLM. The horizontal size of the images is  $374\ \mu\text{m}$

main boundary. Second, the neighboring stripes found in [16–21] have identical structures, whereas in our case, the azimuthal molecular orientation in the adjacent stripes differs: the  $\mathbf{c}$ -director is rotated clockwise with respect to the symmetric orientation in the left stripe (Fig. 4*b,c*) and counterclockwise in the right stripe (Fig. 4*b,c*). Next, inside the stripes investigated in [16–20], the elastic deformation is of the bend type with the same sign of the bend in all stripes and with defect walls in which the  $\mathbf{c}$ -director jumps back. In our case, the reorientation of the  $\mathbf{c}$ -director between stripes is of the splay type. Moreover, there is no visible orientational deformation of the  $\mathbf{c}$ -director inside stripes (Fig. 3*a*). Therefore, care must be taken when comparing published theoretical results with our experimental data. Below, we examine one important aspect of the liquid-crystal modulated phase formation that does not appear to have been investigated in any generality.

In our opinion, the unusual structure of the stripes we have observed is related to the nature of the geometrical frustration in the films formed by a nonchiral material. It was recognized quite some time ago that because of the up–down asymmetry, an achiral smectic film exhibits polar properties and, in particular, the  $\mathbf{c}$ -director may be considered as a true vector (i.e.,  $\mathbf{c}$  and  $-\mathbf{c}$  states are not equivalent). In ferroelectric SmC\* phases, the chiral asymmetry favors a bend ( $\nearrow \rightarrow \searrow$ )

in the  $\mathbf{c}$ -director  $\lambda_b \nabla \times \mathbf{c}$ . The preferred bend direction (the sign of the coefficient  $\lambda_b$  at the term linear in spatial derivatives) is determined by the handedness of the material (or by the direction of the ferroelectric polarization), which is the same in the whole film.

We argue below that in achiral systems, the instability arises from a competition between two elastic energies, the usual quadratic Frank elastic energy, which favors a uniform orientation of the  $\mathbf{c}$ -director, and an additional surface elastic term linear in the  $\mathbf{c}$  gradient, which promotes spontaneous splay distortions. The terms linear in gradients, such as  $\nabla \times \mathbf{c}$ , are not allowed by the symmetry. However, in such a film, the broken chiral symmetry occurs as a result of asymmetry between the surfaces (having hexatic ordering) and the interior of the film (which is in the SmC state). Our measurements show that not only the tilt angle but also the orientational order parameter  $P_2$  differ essentially in SmC and hexatic structures. The surface-induced term linear in the gradients of  $\mathbf{c}$  (proportional to  $\lambda_s \nabla \cdot \mathbf{c}$ ) favors a splay deformation ( $\searrow \uparrow \nearrow$ ) in the  $\mathbf{c}$  field and has the opposite signs (direction of splay curvature) in the top and bottom parts of the film [3, 15]. The  $\mathbf{c}$ -director is also the order parameter of the film. This allows us to describe its macroscopic physics, in particular, to write its free energy in the spirit of the Landau theory as

$$F = \frac{1}{2}K_s(\nabla \cdot \mathbf{c})^2 + \frac{1}{2}K_b(\nabla \times \mathbf{c})^2 + \lambda_s \nabla \cdot \mathbf{c} + \frac{1}{2}A\mathbf{c}^2 + \frac{1}{4}B\mathbf{c}^4. \quad (1)$$

The first two terms are the splay and bend elastic energies, and Frank elastic moduli  $K_s$  and  $K_b$  are proportional to the film thickness. The last two terms are the conventional Landau expansion. The third term  $\nabla \cdot \mathbf{c}$  is a total derivative that can be transformed to boundary terms. Therefore, it is relevant only for thin films. For thick films, another term with the same symmetry can be constructed,

$$\lambda'_s \mathbf{c}^2 \nabla \cdot \mathbf{c}, \quad (2)$$

and to avoid its reduction to a pure surface contribution, variations in the  $\mathbf{c}$  amplitude are needed. These kinds of contributions to the free energy (terms linear in the splay distortion  $\nabla \cdot \mathbf{c}$ ) lead to formation of the unusual modulated structure we have observed in this work.

If the molecules forming the system carried permanent dipole moments  $\boldsymbol{\mu}$  with a nonvanishing component along the direction  $\mathbf{c}$ , then the phase would exhibit a spontaneous electric polarization  $\mathbf{P}$ . This spontaneous polarization is proportional to the polar order parameter. For simplicity and for the lack of different compelling indications from the experimental part of our work, the dipolar forces are neglected in the stripe period estimation below. It might be the case if the molecules involved have relatively large shape anisotropy (and not large electric dipole moment), and ionic impurities screen the Coulomb interaction. This is not the whole story, however. In order to obtain the correct structure of the splay phase, one has to take the complete order parameter, including the modulus  $|\mathbf{c}|$ , into account. There is a price to be paid, because  $|\mathbf{c}|$  cannot be constant where the splay is constant. Indeed, in two-dimensionals, a splay distortion of the orientation cannot occur in a defect-free fashion. Instead, to relieve this frustration, the system forms a modulated phase consisting of a regular network of defect walls and points.

It is interesting and tempting to hypothesize the following stripe structure satisfying such kind of symmetry breaking. The uniform SmC structure of the top part of the film breaks up into finite regions with a splay deformation of the  $\mathbf{c}$ -director (Fig. 4d). Regions with the same favorable sign of the splay (counterclockwise in Fig. 4d) are separated by defect lines in which the  $\mathbf{c}$ -director abruptly rotates back. In the bottom part of the film (Fig. 4e), the  $\mathbf{c}$ -director rotation occurs in the opposite direction (clockwise). The lines in which the

$\mathbf{c}$ -director jumps back are shifted in the  $x$ -direction by the stripe period  $d_{st}$  with respect to the top part of the film (Fig. 4d,e). In this structure, the direction of the splay modulation in  $\mathbf{c}$  is favorable on both sides of the film. Remarkably, the net magnitude of the  $\mathbf{c}$ -director orientation  $\varphi$  across the film is constant in each stripe in the agreement with our experimental data. Their values  $\varphi = \pm 15^\circ$  are dictated by the structure of the surface SmL phase. To be stable, a splay-modulated structure has to overcome the unfavorable core defect energy ( $\varepsilon$ ) and the ordinary nematic order parameter contribution. In the zeroth approximation, the periodic stripe phase exists when the gain in the surface elasticity energy exceeds the domain wall energy  $\varepsilon$ . Competition between these energies determines the stripe width as [15]

$$D_{st} \approx \frac{K}{\lambda_s - \varepsilon}, \quad (3)$$

where  $K = (K_s + K_b)/2$  is the mean Frank constant. In the temperature window  $T > T_C$  (where  $T_C$  is the bulk SmC–HSmB transition temperature) in which we are interested, the main temperature-dependent factor in (3) is  $\lambda_s$ . The very existence of this linear splay distortion is due to the asymmetry of the order parameter profile over the film. Induced by the surface ordering  $\Psi_s$ , the hexatic (bond) order parameter  $\Psi$  decays toward the interior of the film as

$$\Psi(z) \propto \Psi_s \frac{\text{ch}[(z - L)/\xi]}{\text{ch}(L/\xi)}, \quad (4)$$

where  $L = Nd$  is the film thickness,  $d$  is the layer thickness, and  $\xi$  is the bulk phase transition correlation length

$$\xi \approx \frac{\xi_0}{\sqrt{(T - T_C)/T_C}}, \quad (5)$$

with  $\xi_0$  denoting the bare microscopic correlation length. The asymmetry of the profile  $\Psi$  determines the value of the parameter  $\lambda_s$ ,

$$\lambda_s = \lambda_0 \text{th} \frac{L}{\xi}, \quad (6)$$

and the transition from the homogeneous to the modulated phase occurs if the asymmetry is sufficiently strong (see (3)). Equations (3)–(6) allow comparing the experimental dependence of the stripe period on temperature (Fig. 5) with theory and determining the parameters of the theory, namely  $\lambda_0/K$  and  $\varepsilon/K$ . We took  $\xi_0/d = 0.5$  and treated  $\lambda_0/K$  and  $\varepsilon/K$  as the fitting parameters. The solid line in Fig. 5 corresponds

to  $\lambda_0/K = 0.95 (\mu\text{m})^{-1}$  and  $\varepsilon/K = 0.61 (\mu\text{m})^{-1}$ . Thus determined,  $\lambda_0/K$  and  $\varepsilon/K$  allow us to make the following estimations. Using the value of the splay elastic constant  $K$  in smectic liquid crystals  $3 \cdot 10^{-6}$  erg/cm [22], we obtain  $\lambda_0 = 2.9 \cdot 10^{-2}$  erg/cm<sup>2</sup> and  $\varepsilon = 1.8 \cdot 10^{-2}$  erg/cm<sup>2</sup>. These values of  $\lambda_0$  and  $\varepsilon$  denote the energy per unit thickness. For films,  $\lambda_0$  and  $\varepsilon$  must be multiplied by  $L$ . We note that for thin films, the continuous approximation used in (4)–(6) is not completely correct and the above values of  $\lambda_0$  and  $\varepsilon$  should be considered as estimations. For a more precise analysis, discrete models of smectic films must be used. We finish with the conclusion that the stripe phase (soliton regime) appears spontaneously on cooling and then the distortion period increases with decreasing the temperature. The theoretical consideration conforms to our experimental observations.

We observe complex phase behavior with various equilibrium structures. A separate question how to calculate all equilibrium structures of a specific system requires full minimization of the global free energy, and it depends on the unknown phenomenological Landau expansion coefficients. We do not even attempt the calculation of such a complex phase diagram in this paper, but content ourselves with one remark. Modulated phases we found have nonuniform density or orientation distributions, that is to say, their symmetry is that of a solid or a liquid crystal. The difference between the phases that appear under the name of modulated structures, on the one hand, and solids or liquid crystals on the other hand, is that the modulation period in the former is generally larger than in the latter.

#### 4. CONCLUSION

It is not a major goal of this work to achieve quantitative agreement between the results obtained with our phenomenological model and experimental measurements. However, because the present understanding of the mechanism leading to modulated structures in achiral tilted hexatic films is incomplete, the model may be an appropriate tool for working out typical trends that may be testable in experiments. In this paper, we have presented results of studies of structural transformations in thin liquid-crystal films with the transition from the smectic- $C$  (Sm $C$ ) to hexatic (HSm $B$ ) phase, and their interpretation within a simple phenomenological model. The free energy was written in the simplest form that involves the least number of model parameters, and we have shown that this simple model can capture many features seen in ex-

periment. Our interpretation of the results is based on the simple consideration that because of the up-down asymmetry, the achiral smectic film exhibits polar properties. One note of caution is in order here. In fact, the structure of any Sm $C$  phase is inherently polar because the tilt singles out a unique direction about the layer normal  $\nu$  (although the directors  $\mathbf{n}$  and  $-\mathbf{n}$  are physically indistinguishable). Therefore, in the Sm $C$  structure, one may have the pseudo-vector

$$\mathbf{l} = (\nu \times \mathbf{n})(\nu \mathbf{n}). \quad (7)$$

Obviously,  $\mathbf{l}$  is perpendicular to the tilt plane, and this kind of polarity (along the pseudo-vector  $\mathbf{l}$ ) is of a fundamentally different nature compared with the polarity along  $\mathbf{c}$  that we investigated in this paper. Indeed, the  $\mathbf{l}$  polarity is compatible with mirror symmetry in the tilt plane, whereas the polar splay distortion responsible for the stripe structure changes its sign under such a mirror reflection.

A question of primary importance is to understand the origin of the thermodynamic behavior we found in this work. It is well known [23] that for a film with the uniform ordering (like nematic or ferromagnetic), when the interaction at the boundaries is such that it enhances local order, a surface transition may occur at temperatures above the critical temperature of the bulk. In such a transition, the layers close to the surface become ordered, although the bulk remains disordered. Depending on the nature of the interactions between the bulk and the surface, the system may exhibit various surface phase transitions, for instance, wetting transitions. In that case, at temperatures just below the bulk transition, the thickness of the surface-ordered layer is infinite. But nonuniformly ordered (modulated) systems do not necessarily exhibit wetting phenomena in which the thickness of the surface-ordered layer diverges. Instead, the system might exhibit a transition from one surface state to another, where both surface states have a finite thickness [11]. Because we consider modulated (nonuniform) structures in this work, the aforesaid arguments provide a physically appealing thermodynamic interpretation of our results.

First of all, because we deal with films, the basic thermodynamics of phase transitions should be formulated for this kind of restricted geometry. Such a problem was discussed for various systems long ago, and the results borrowed from textbooks [23, 24] are as follows. In a film of thickness  $L$ , the thermodynamic potential  $G$  per unit area is

$$\frac{G}{A} = -pL + 2\gamma, \quad (8)$$

where  $\gamma$  is the surface free energy,  $p$  is the bulk pressure, and  $A$  is the area. We let the surface free energies of the smectic  $C$  and hexatic phases be denoted by  $\gamma_C$  and  $\gamma_H$  respectively. The Laplace condition then yields

$$\gamma_C = \gamma_H + \gamma_{C-H} \cos \theta, \quad (9)$$

where  $\theta$  is the contact angle between  $\text{Sm}C$  and hexatic phases and  $\gamma_{C-H}$  is the surface energy at the interface. In the bulk, the coexistence temperature  $T_C$  is determined by the equilibrium condition

$$p_C(T_C) = p_H(T_C). \quad (10)$$

In a film of a finite thickness  $L$ ,

$$T_m = T_C + \Delta T(L), \quad (11)$$

and from  $G_C = G_H$  we find

$$-p_H(T_m) + \frac{2\gamma_H}{L} = -p_C(T_m) + \frac{2\gamma_C}{L}. \quad (12)$$

Because

$$p = p(T_C) + S(T_C)\Delta T \quad (13)$$

(where  $S$  is the entropy), we obtain

$$\Delta T(L) = \frac{2(\gamma_C - \gamma_H)T_C}{LQ}, \quad (14)$$

and  $Q = T_C(S_C - S_H)$  is the latent heat at the bulk transition. Equation (14) can be equivalently expressed (see (9)) as

$$\Delta T(L) = \frac{2T_C\gamma_{C-H} \cos \theta}{LQ}. \quad (15)$$

However, in (14), we did not consider the interaction  $\Pi(L)$  [25] between the film surfaces (or between the walls). Repeating the same thermodynamical analysis, we obtain an equation of the same kind but with the surface energy  $\gamma$  renormalized by the disjoining pressure  $p_d$  [25],

$$2\tilde{\gamma}(L) = 2\gamma + Lp_d + \Pi. \quad (16)$$

According to (15), at the contact angle  $\theta = 0$ , the  $\text{HSm}B$  phase is favored near the boundary and  $\theta = \pi$ , the  $\text{Sm}C$  phase is favored, and the intermediate values of  $\theta$  apply to intermediate structures. In any case, for a finite film thickness, there are two possible scenarios depending on the film thickness. In one scenario, the phase transition occurs before the surface  $\text{HSm}B$  layer has had a chance to grow thick. In the other scenario, a phase transition can occur at a temperature at which

the  $\text{HSm}B$  thickness at the surface is already larger than the sample thickness  $L$ .

Clearly, there are several open questions and future challenges. One of them is related to dipolar forces. Indeed, because the molecules are tilted and the interface and the interior symmetry of the film are different from each other, the film has only one symmetry element, the vertical mirror plane, which is perpendicular to the film and parallel to the molecules. The film is therefore equivalent to a two-dimensional polar nematic, and it bears an electric polarization. If this polarization is small compared to the elastic energies involved, our arguments given above apply. On the other hand, if electric energies dominate, another kind of texture can be stable, because all splay centers act as charge centers, and a lattice of several small charges is then more stable than one big charge. Another interesting question is how to tune parameters of the various modulated structures to optimize properties of technological interest. For instance, a wide area of research is clearly the problem to what extent the investigated systems can be useful to achieve interesting electro-optical properties. The treatment above can be generalized to more realistic systems (e.g., dipolar forces including), with the same conceptual ingredients, albeit at the expense of a rapidly increasing complexity.

This work was supported in part by the RFBR (grant № 05-02-16675), Program of RAS Presidium «Influence of Atomic and Crystalline Structure on Properties of Condensed Media», and by Grant of the President of Russia MK-4057.2005.2. One of us (E. I. K.) acknowledges support from INTAS (under № 01-0105) Grants.

## REFERENCES

1. T. Stoebe and C. C. Huang, *Int. J. Mod. Phys.* **9**, 2285 (1995).
2. W. H. de Jeu, B. I. Ostrovskii, and A. N. Shalaginov, *Rev. Mod. Phys.* **75**, 181 (2003).
3. J. Maclennan and M. Seul, *Phys. Rev. Lett.* **69**, 2082 (1992).
4. J. E. Maclennan, U. Sohling, N. Clark, and M. Seul, *Phys. Rev. E* **49**, 3207 (1994).
5. E. I. Demikhov and V. K. Dolganov, *Pis'ma v Zh. Eksp. Teor. Fiz.* **64**, 29 (1996) [*JETP Lett.* **64**, 32 (1996)].
6. C. Y. Chao, T. C. Pan, and J. T. Ho, *Phys. Rev. E* **67**, 040702(R) (2003).

7. M. Born and E. Wolf, *Principles of Optics*, Pergamon Press, New York (1983).
8. D. R. Link, G. Natale, R. Shao, N. A. Clark, E. Korbulova, and D. M. Walba, *Science* **84**, 3665 (1999).
9. L. M. Blinov, *Electro-Optical and Magneto-Optical Properties of Liquid Crystals*, Wiley, New York (1983).
10. S. Heinekamp, R. A. Pelcovits, E. Fontes, E. Yi. Chen, and R. Pindak, *Phys. Rev. Lett.* **52**, 1017 (1984).
11. M. Seul and D. Andelman, *Science* **267**, 476 (1995).
12. P. O. Andreeva, V. K. Dolganov, C. Gors, R. Fouret, and E. I. Kats, *Pis'ma v Zh. Eksp. Teor. Fiz.* **67**, 808 (1998) [*JETP Lett.* **67**, 856 (1998)].
13. P. O. Andreeva, V. K. Dolganov, C. Gors, R. Fouret, and E. I. Kats, *Phys. Rev E* **59**, 4143 (1999).
14. D. R. Link, G. Natale, J. E. Maclennan, N. A. Clark, M. Walsh, S. S. Keast, and M. E. Neubert, *Phys. Rev. Lett.* **83**, 3665 (1999).
15. R. B. Meyer and P. S. Pershan, *Sol. St. Comm.* **13**, 989 (1973).
16. D. Blankschtein and R. M. Hornreich, *Phys. Rev. B* **32**, 3214 (1985).
17. S. A. Langer and J. P. Sethna, *Phys. Rev. A* **34**, 5035 (1986).
18. G. A. Hinshaw and R. G. Petschek, *Phys. Rev. A* **39**, 5914 (1989).
19. J. V. Selinger, Z. G. Wang, R. F. Bruinsma, and C. M. Knobler, *Phys. Rev. Lett.* **70**, 1139 (1993).
20. R. D. Kamien and J. V. Selinger, *J. Phys.: Condens. Matter* **13**, R1 (2001).
21. N. Vaupotič and M. Čopič, *Phys. Rev. E* **72**, 031701 (2005).
22. P. V. Dolganov and B. M. Bolotin, *Pis'ma v Zh. Eksp. Teor. Fiz.* **77**, 503 (2003) [*JETP Lett.* **77**, 429 (2003)].
23. K. Binder, *Phase Transitions and Critical Phenomena*, ed. by C. Domb and J. L. Leibowitz, Vol. 8, Acad. Press, London (1986).
24. L. D. Landau and E. M. Lifshits, *Statistical Physics*, part 1, Pergamon, Oxford (1980).
25. F. Picano, P. Oswald, and E. Kats, *Phys. Rev. E* **63**, 021705 (2001).